

© Terra/EOS AM-1

Automatically dunes mapping and morphometric analysis using Artificial Intelligence

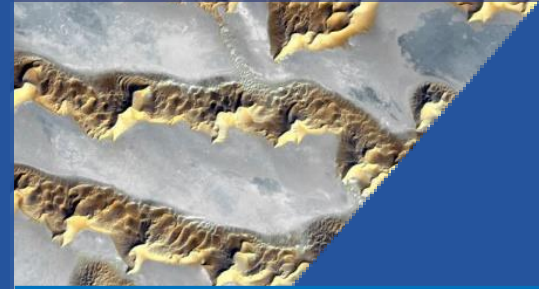
Jimmy Daynac^{1}, Paul Bessin¹, Stéphane Pochat², and Régis Mourgues¹*

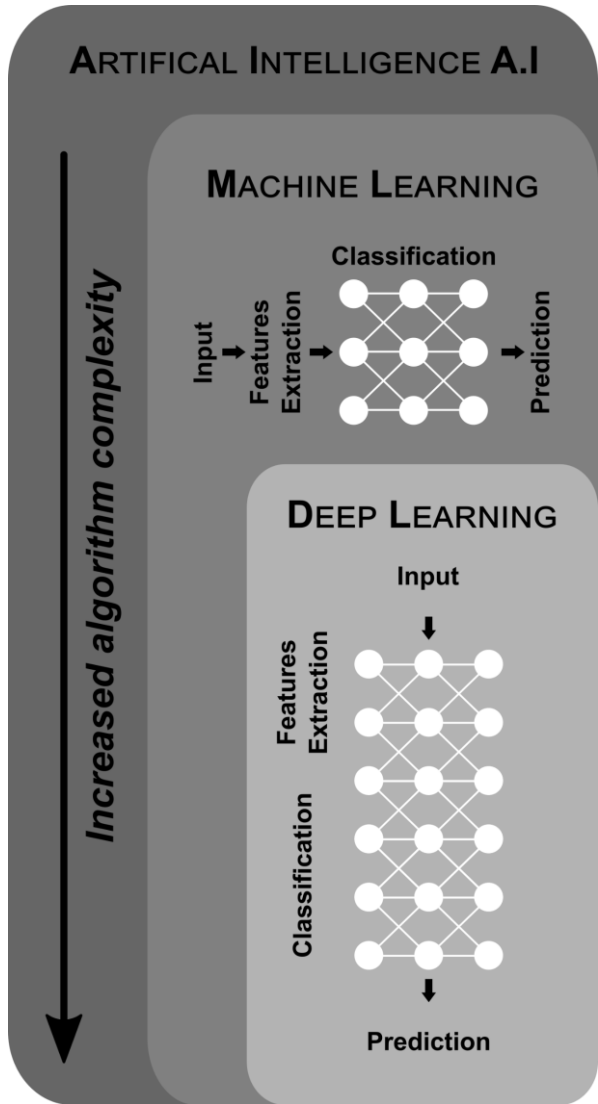
¹UMR 6112 LPG, Le Mans Université, Le Mans, France (jimmy.daynac@univ-lemans.fr)

²UMR 6112 LPG, Nantes Université, Nantes, France

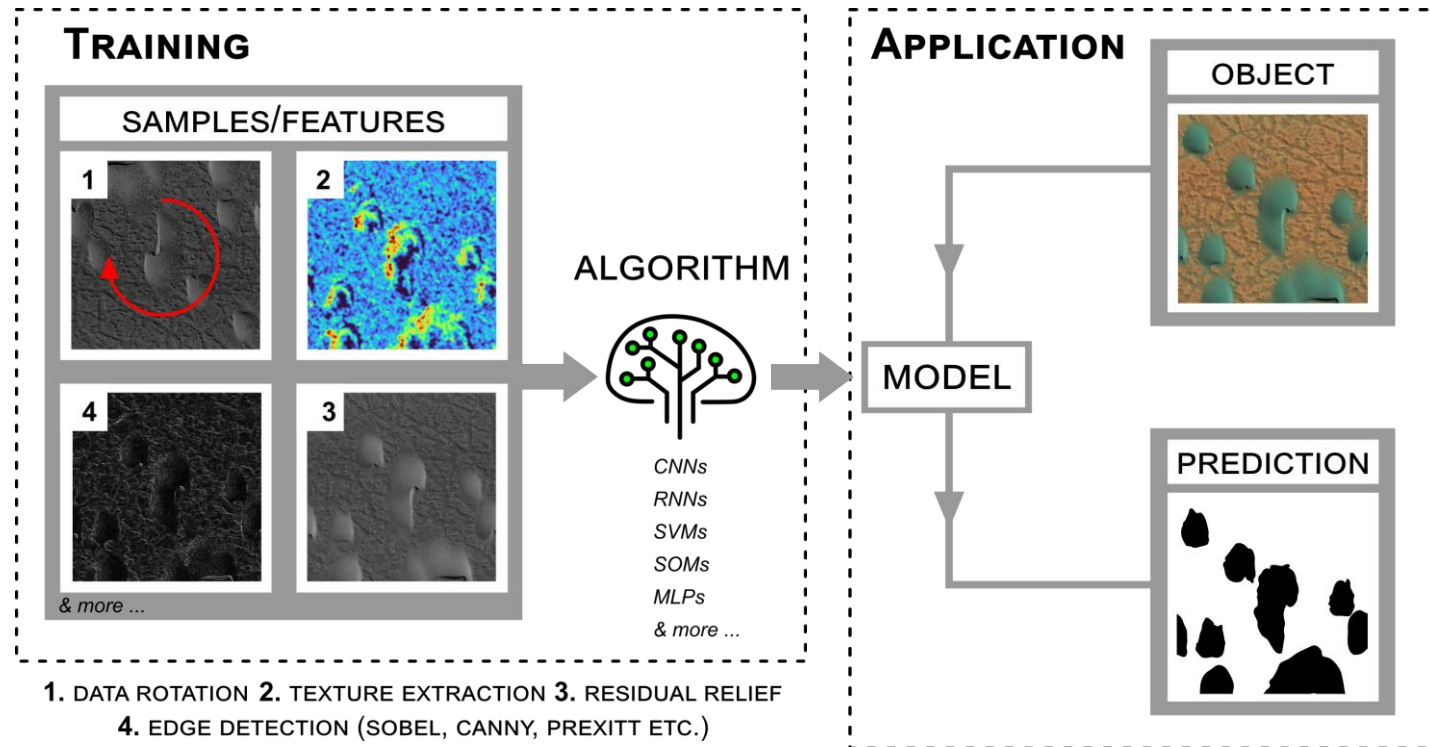


DOCTORAT ECOLOGIE
BRETAGNE GEOSCIENCES
LOIRE AGRONOMIE ALIMENTATION

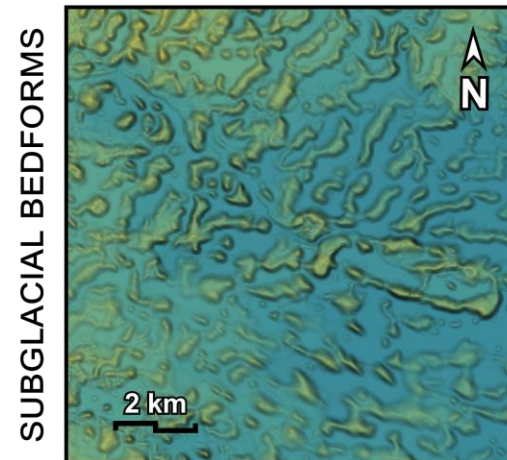
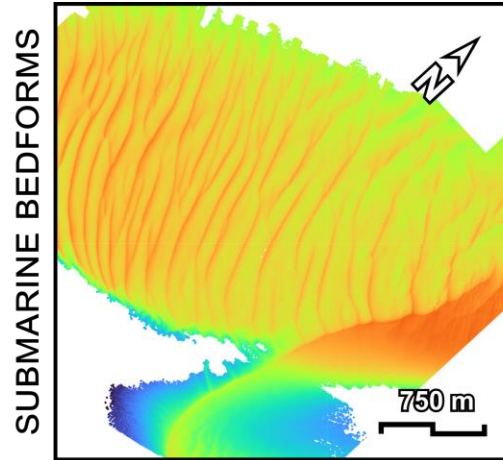
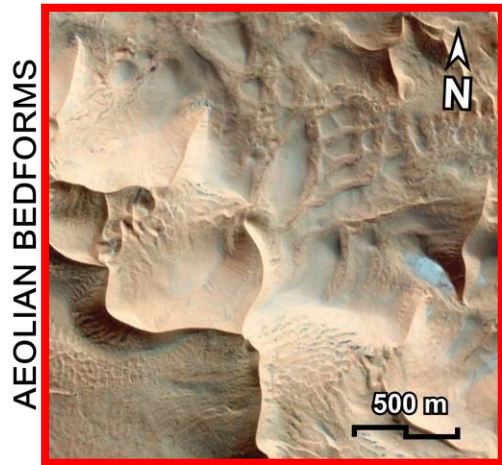




Artificial Intelligence (A.I): Scientific domain that seeks to solve logical or arithmetic problems by mimicking the decision-making capacity of a human brain.

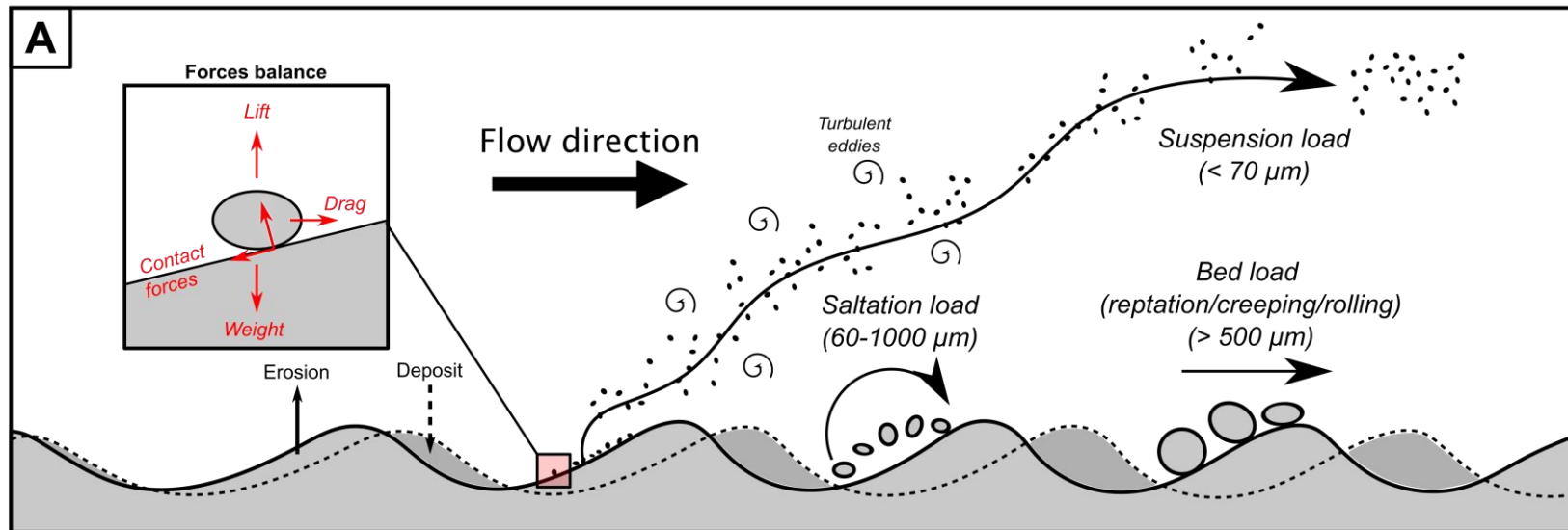


Interest



Bedforms: spatially organized periodic patterns formed by the flow of a fluid on a substrate and by different processes of material mobilization.

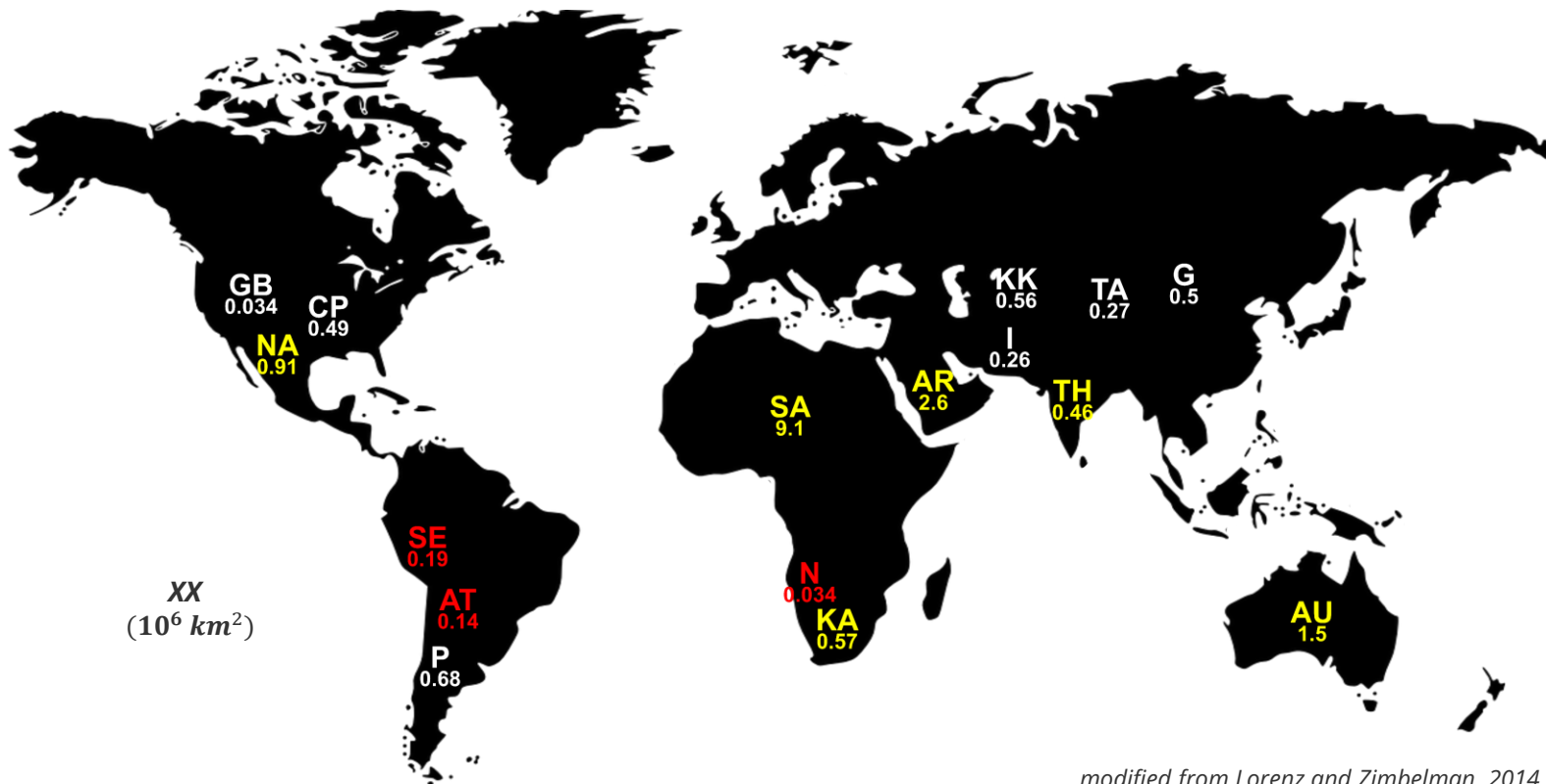
Granular transport



Bed load
(reptation + creeping + rolling)

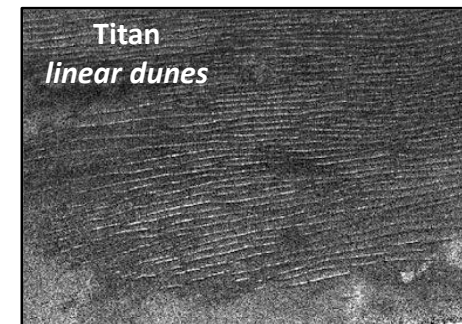
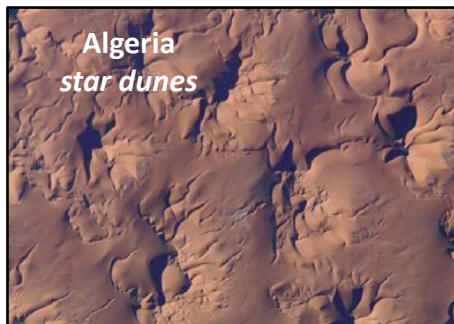
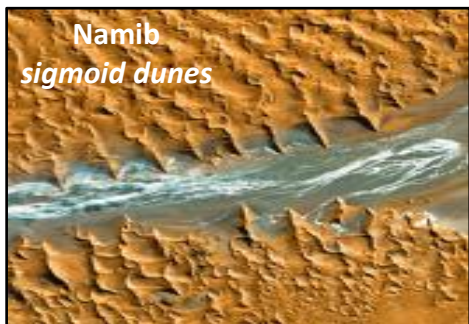
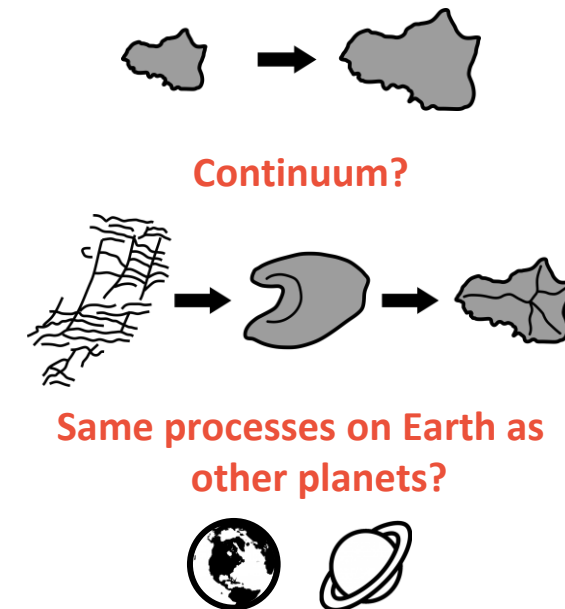
Saltation load

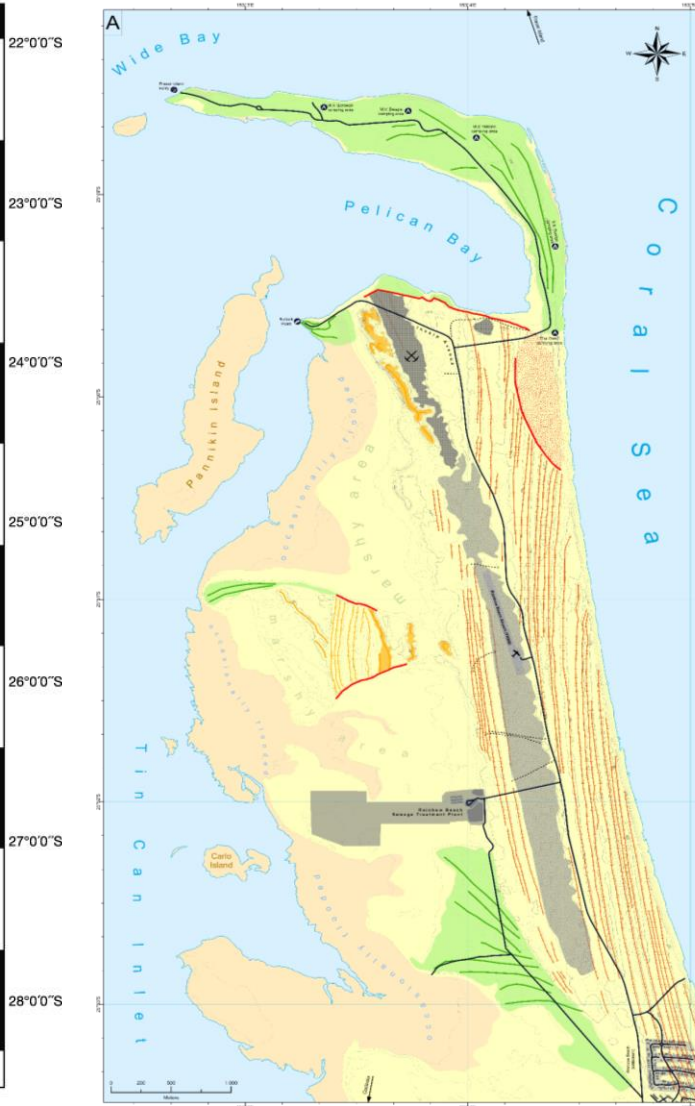
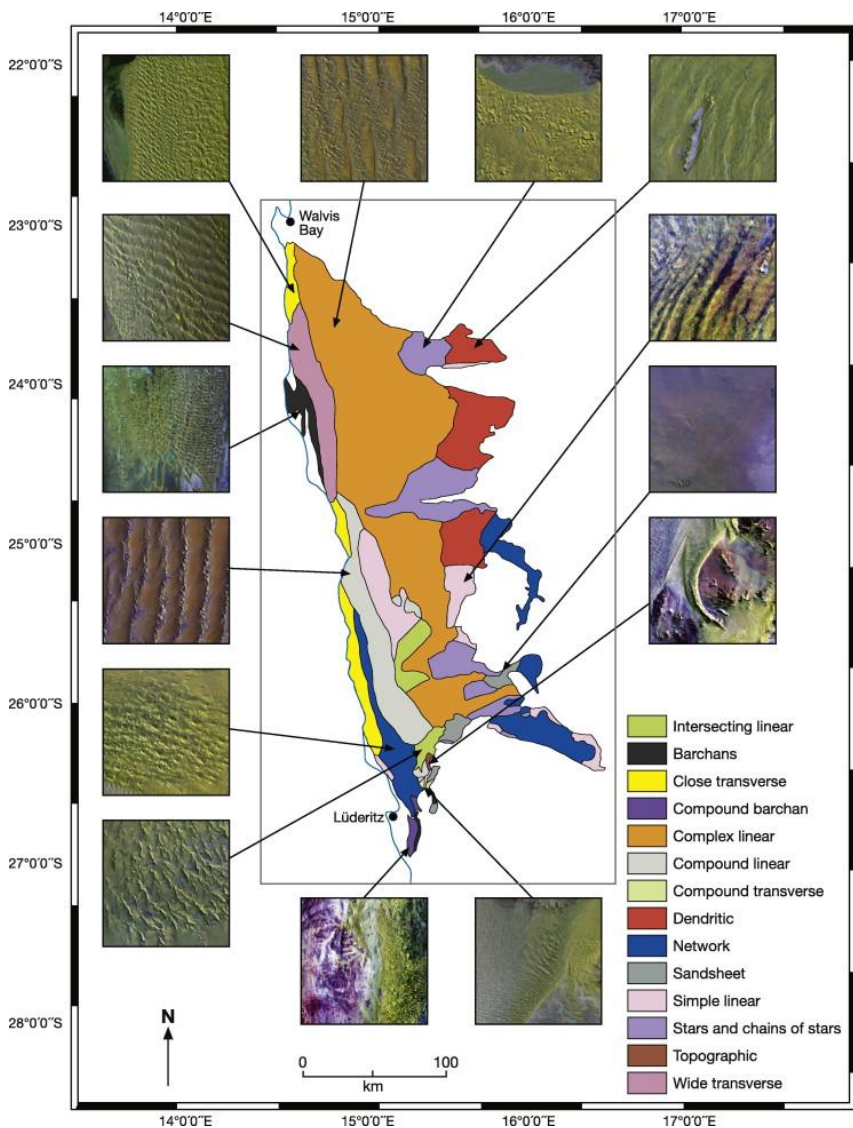
Suspension load



modified from Lorenz and Zimbelman, 2014

Some different forms/sizes/spacing

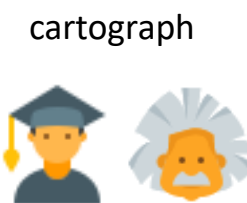
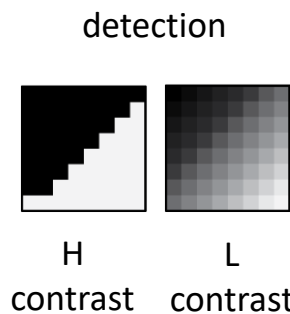
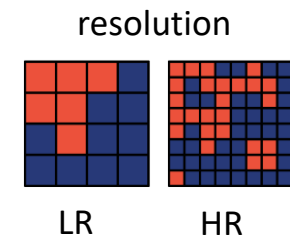


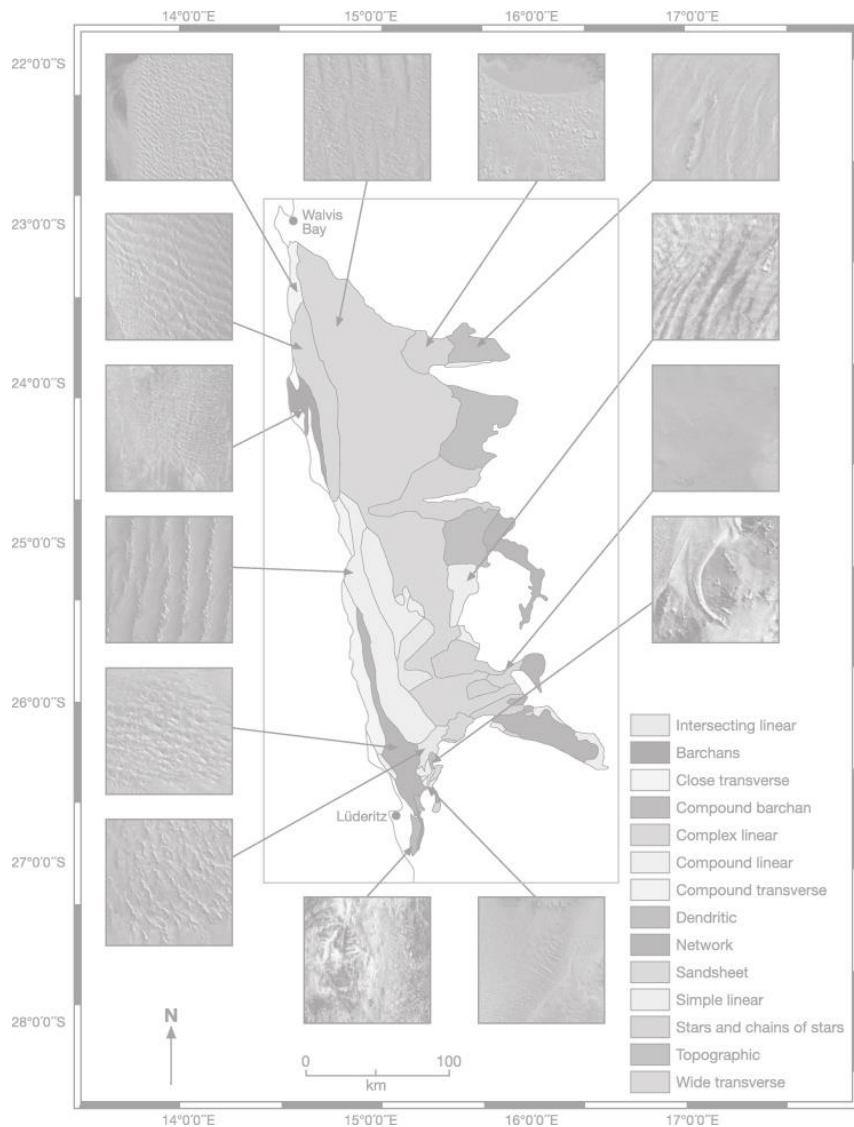


Problems

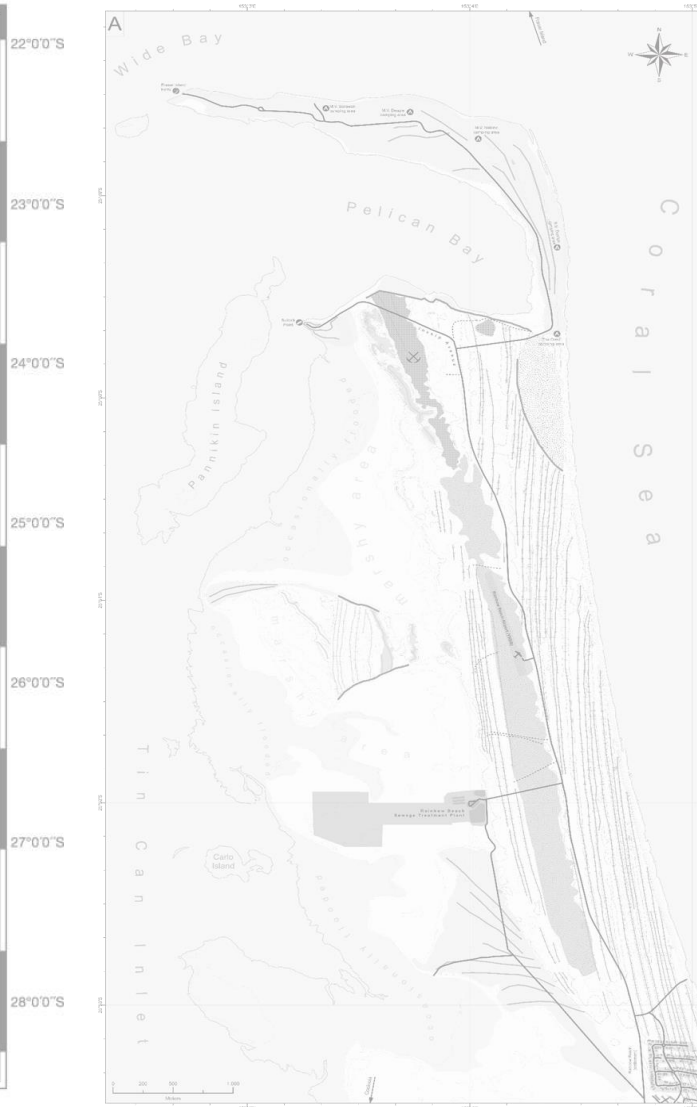


Manual bias





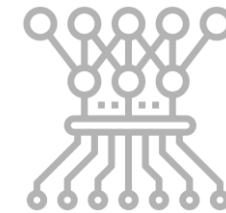
Livingstone, 2010



Köhler et al., 2021

How to map quickly and accurately ?

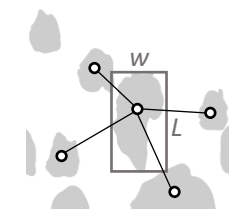
- 1 Develop an automated mapping protocol



- 2 Create a vector dunes database



- 3 Quantify dune geometry





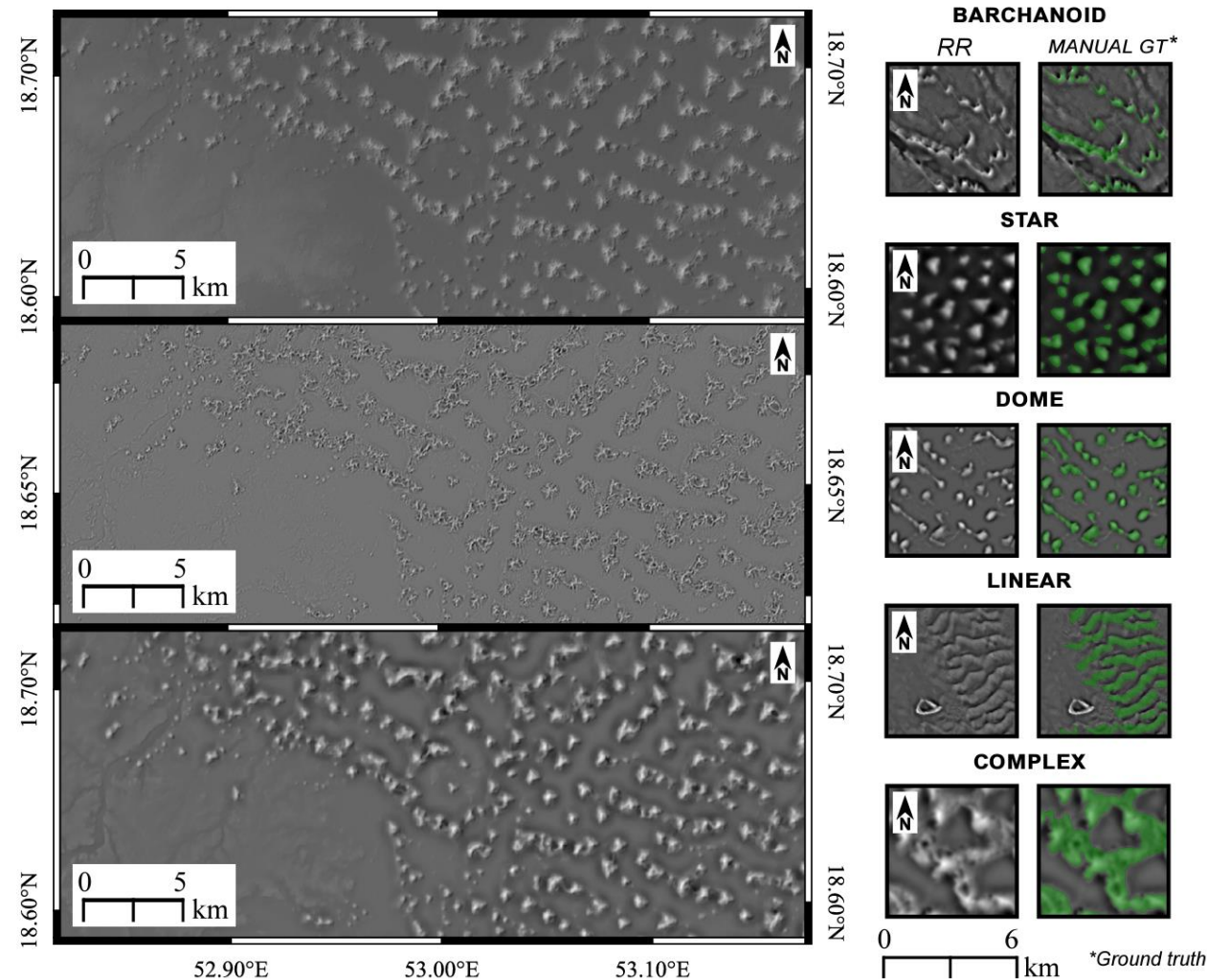
Sharing not permitted

Residual Relief (RR) computation and sampling

Dune fields show superimposed generations of dunes (m to km-scale) producing complex topographic signal on DEMs. Each dune scale patterns can be analyzed independently if the topographic signal is disentangled with the Residual Relief approach (Hiller and Smith, 2008).

We computed it on 100 training samples that are then used as learning data set to map the dune outlines.

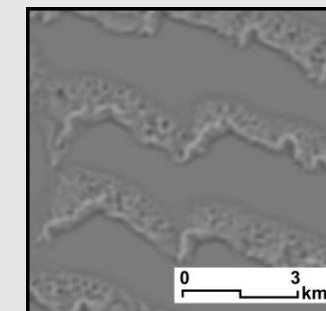
The samples are selected from four arid regions and cover a large range of dune types (barchanoid, star, dome, linear and complex dunes). Each sample represent a DEM on which dunes are identified and digitalized manually. This manual mask is considered as a "ground truth" reference by the Deep Learning algorithm.



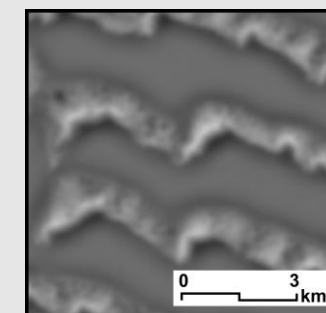
Daynac et al., (in prep)

OUTPUT VISUEL

Short generation



Large generation



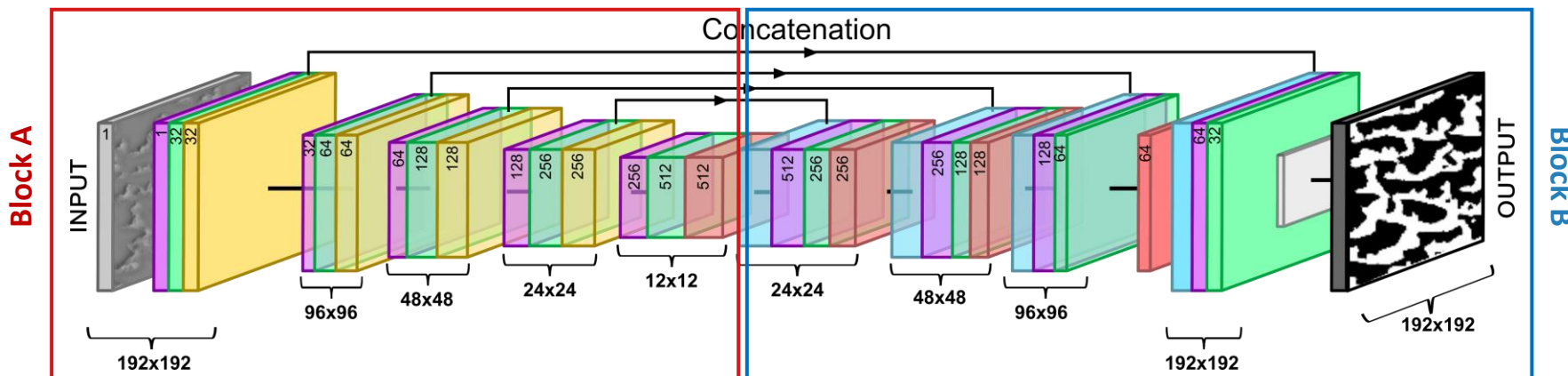
Deep Learning algorithm - Convolutional neural network (CNN) training

The CNN is a robust algorithm to detect the bedform shapes in a landscape and produce a binary raster of this interest objects (DeLatte et al., 2019; Shumack et al., 2020).

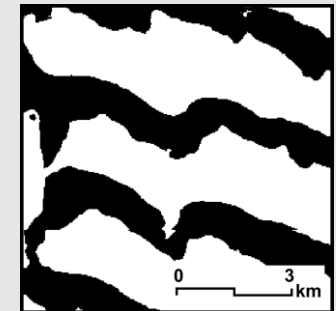
The CNN architecture is based on the assemblage of a contraction path (block A) and an expansive path (block B), each path is characterized by two phases of convolutions.

Convolution is a mathematical matrix operation that consists of multiplying the values associated with the features of interest (here the contour of the dunes) by a kernel filter (for example the contour detection filter). This process is repeated until the entire image is filtered. The sum of the matrices products generates an image of a smaller resolution.

The convolution steps are followed by different matrix operations of maxpooling, convolution transpose and concatenation that allow us to summarize and localize on the image all values associated with our objects of interest.



OUTPUT VISUEL



Recall
87%

Accuracy
91%

Quality
70%

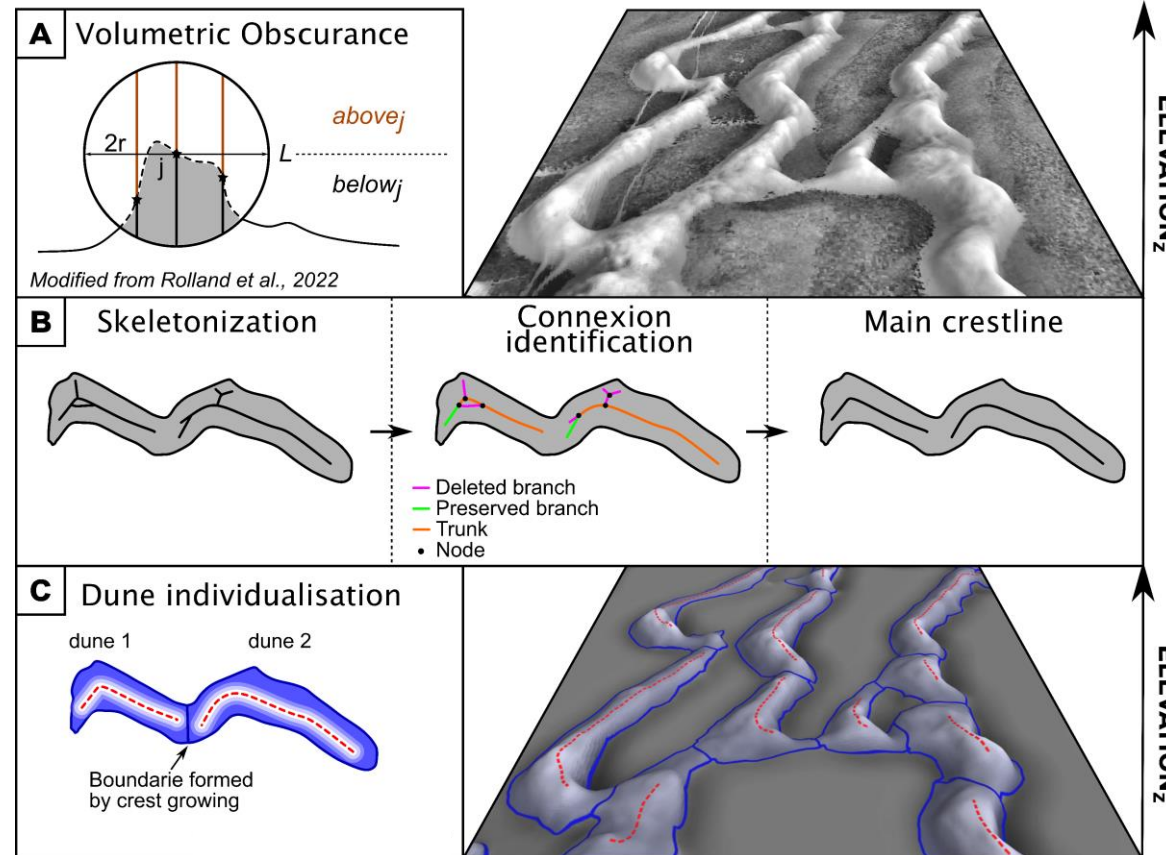


Sharing not permitted

Crestlines extraction

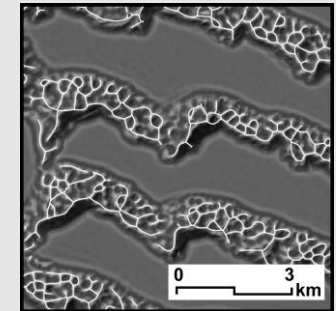
The crestlines extraction is based on the Volumetric Obscure algorithm (Rolland et al., 2022). The tool calculates for each pixel on a DEM the ratio between the volume below and above the topography in a sphere of a given radius centered at a given point of the topographic surface.

The output raster is reduced to a branched skeleton from our automated algorithm that analyzes the branch connectivity of each bedform crestlines to keep the longest segment defined as the main crestline of a dune.

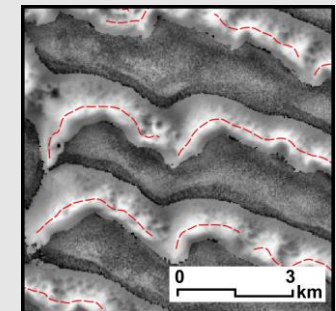


OUTPUT VISUEL

Short generation



Large generation



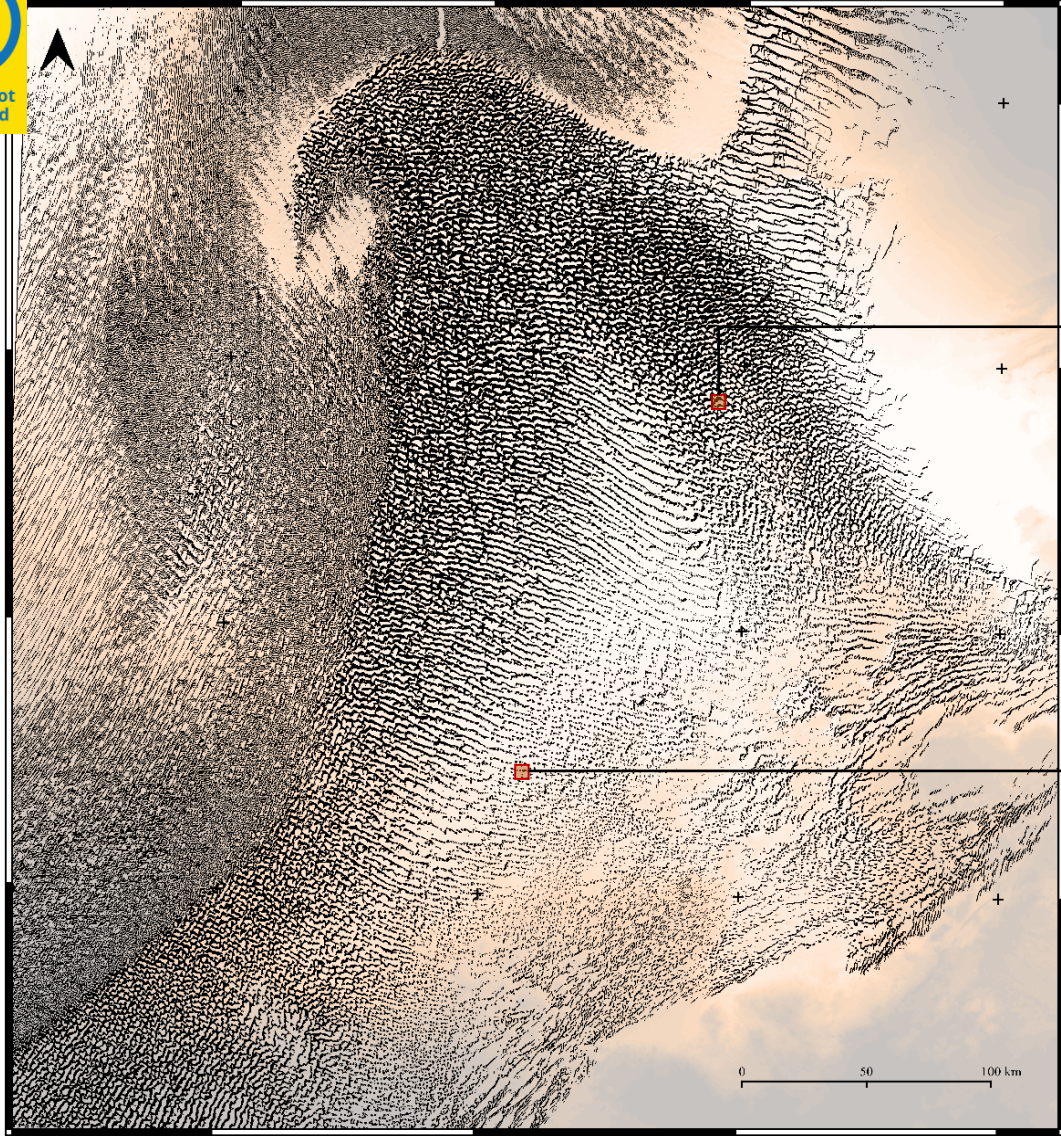
Daynac et al., (in prep)



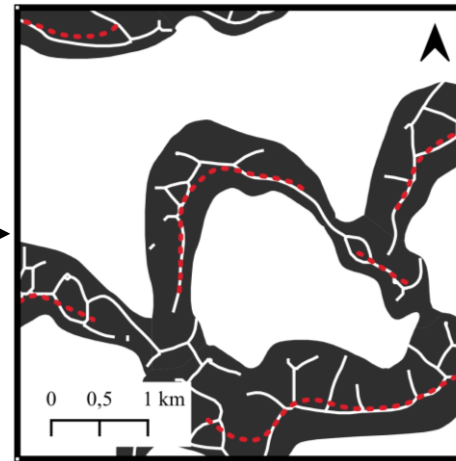
53.0°E 54.0°E 55.0°E 56.0°E

Daynac et al., (in prep)

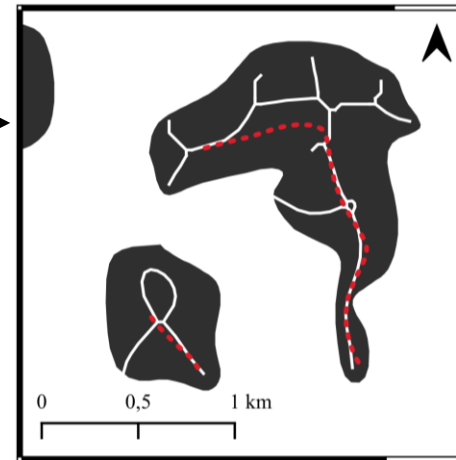
22.0°N
21.0°N
20.0°N



Barchanoid dunes







Star dunes



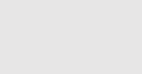


Rub'Al Khali dune field map

Numerical metrics

-  6:00
-  78,000 individualized dunes & crestlines
-  1,280,000 superimposed crest segments
-  58,000 km²

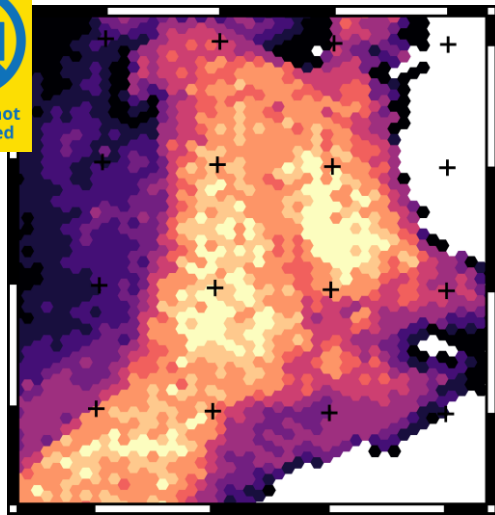
Legend

-  Dune outline
-  Crest of 2^{sd} dune generation superimposed
-  Main crest

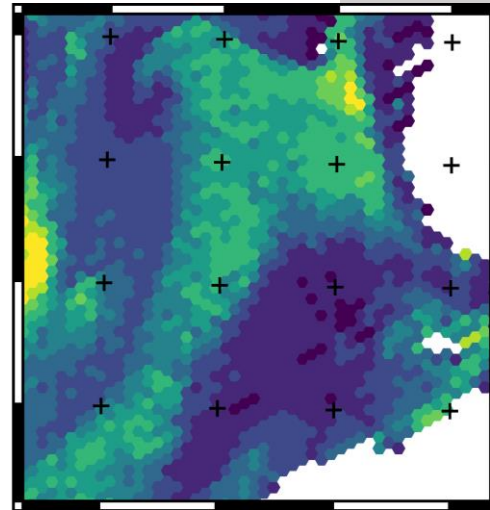
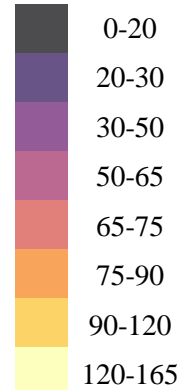
Daynac et al., (in prep)



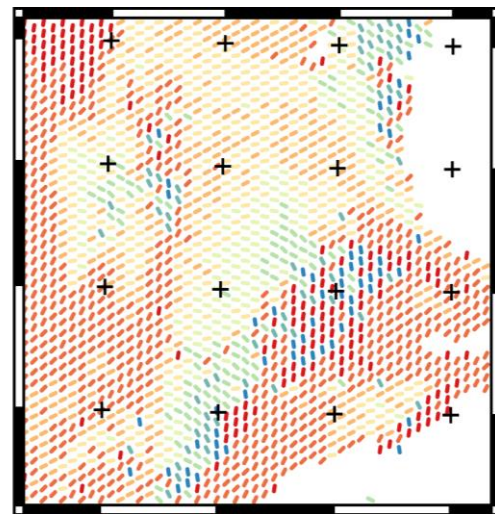
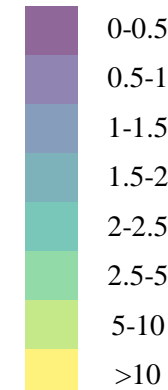
Daynac et al., (in prep)



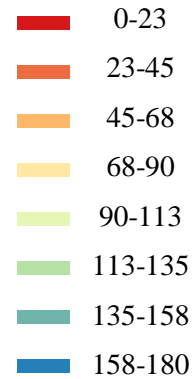
HEIGHT_{DUNE} (m)



LENGTH_{DUNE} (km)



DIRECTION_{CREST} (°)

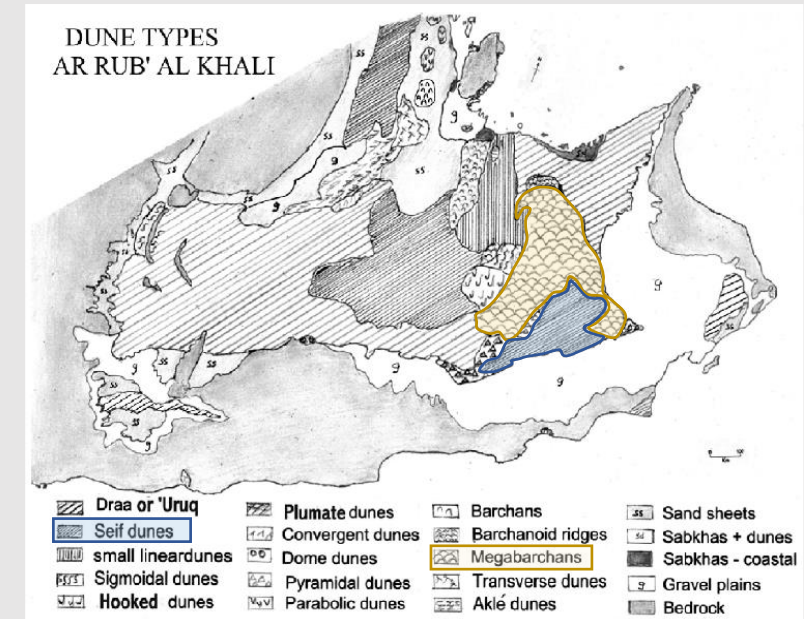


This is one of the first detailed maps of morphometric parameters of the Rub'Al Khali dunes showing:

- Mean crestlines direction of 81°(range: 45°-135°) for high dunes (>70m) and of 35° (range: 171°-180°) for smaller dunes (<70m);
- A central area with a very consistent pattern of long (>2 km) and high (> 70m) dunes;
- A south area with a very consistent pattern of shorter (< 1 km) and a height gradient that decreases to the south (70 to 20m);
- A similarity between the central area pattern of our work and the megabarchan area identified at the dune field scale in previous studies;
- A similarity between the south area pattern of our work and seif dunes area identified at the dune field scale in previous studies.

Morphometric parameters of Rub'Al Khali dunes

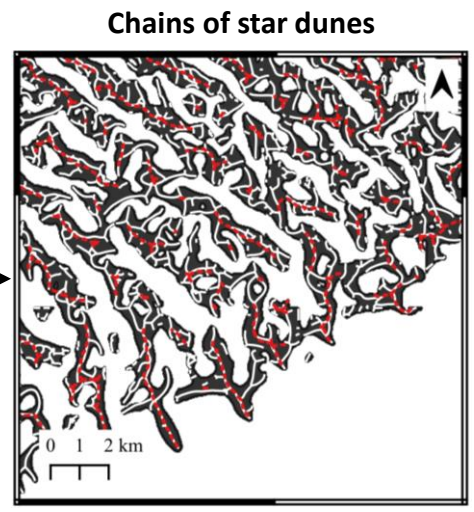
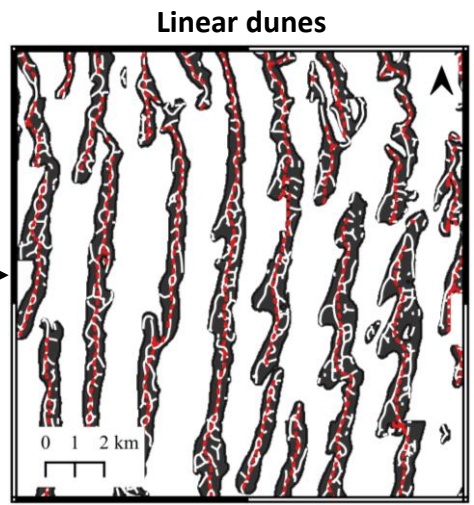
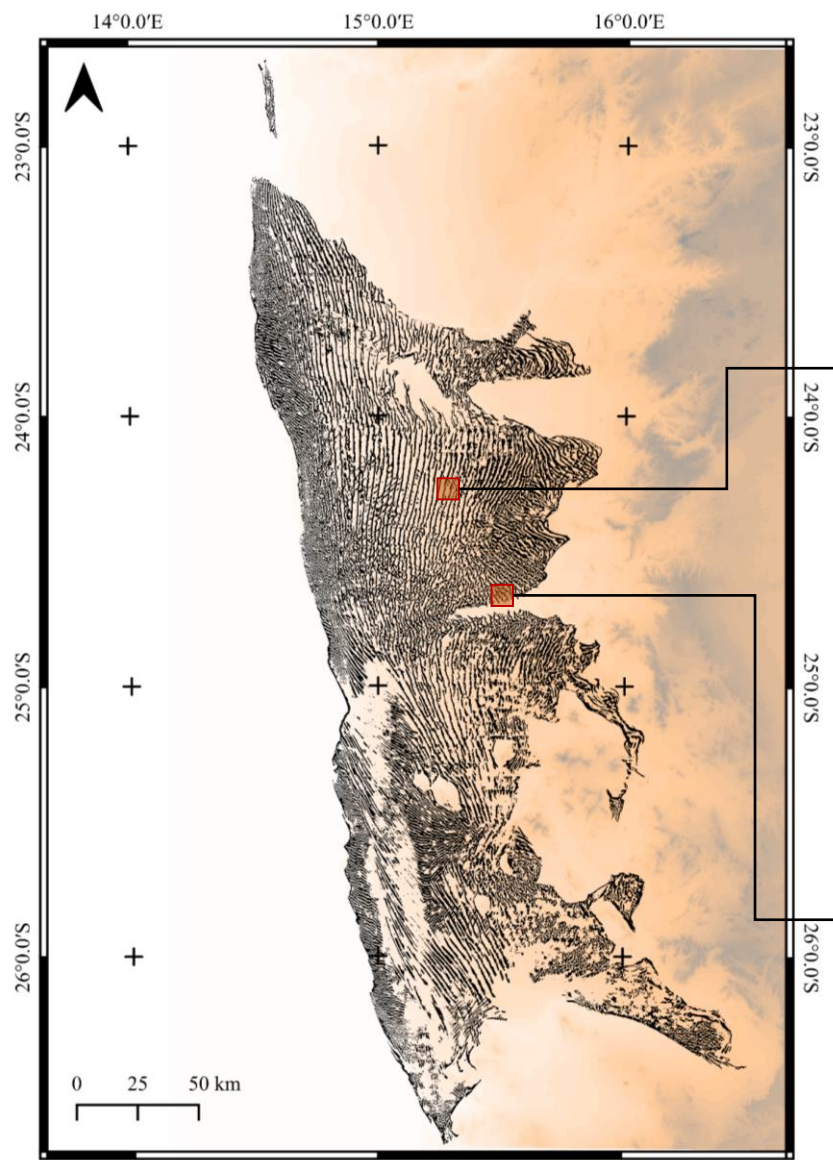
Comparison with current map



modified from Edgell, 2006







Daynac et al., (in prep)






Namib dune field map

Numerical metrics

-  5:00
-  17,000 individualized dunes & crestlines
-  228,198 superimposed crest segments
-  12,000 km²

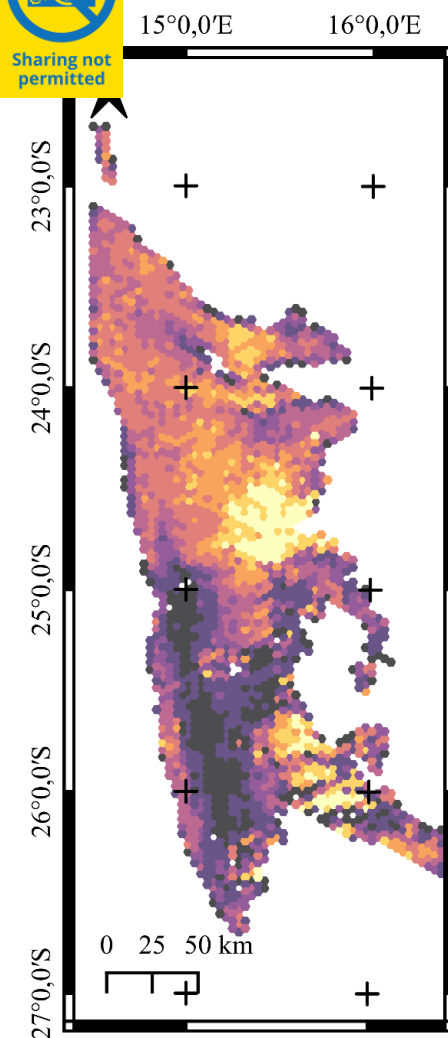
Legend

-  Dune outline
-  Crest of 2nd dune generation superimposed
-  Main crest

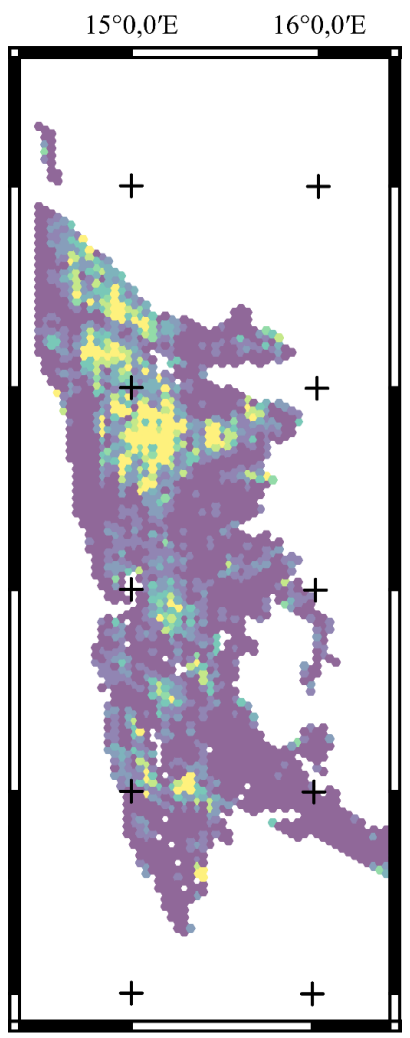
Morphometric parameters of Namib dunes



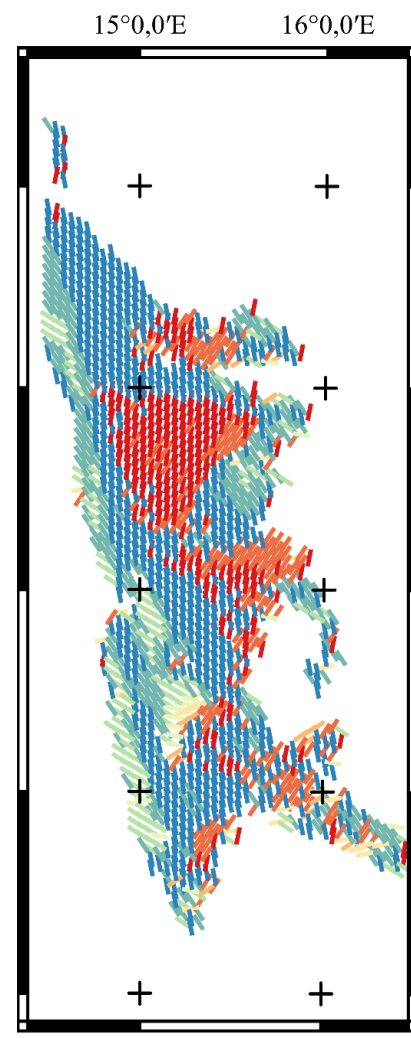
Sharing not permitted



HEIGHT_{DUNE} (m)



LENGTH_{DUNE} (km)

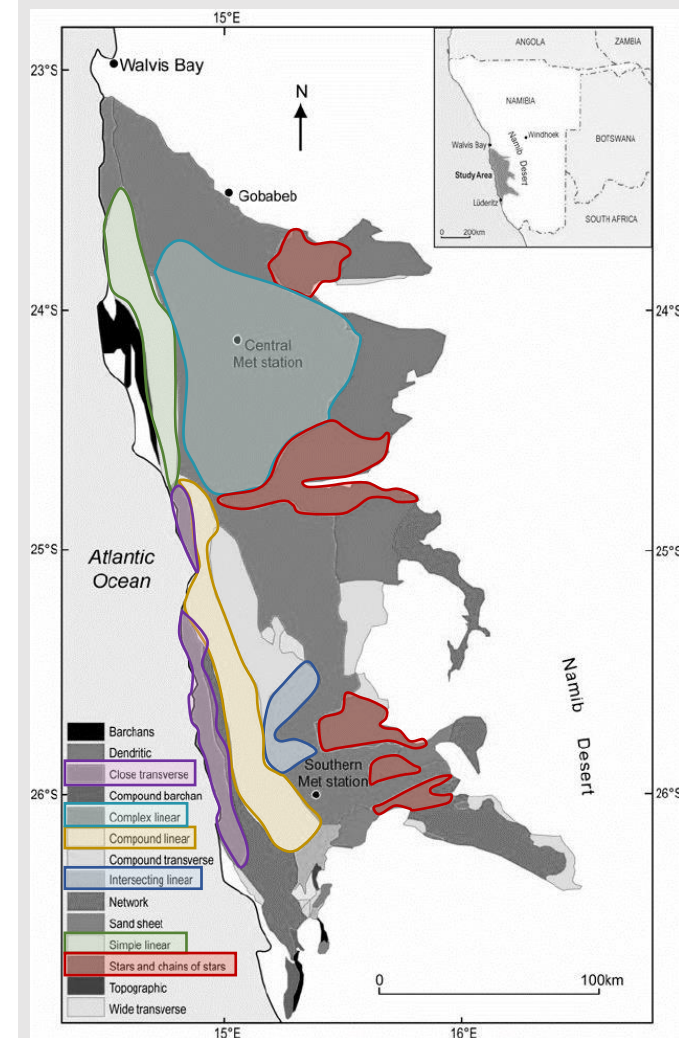


DIRECTION_{CREST} (°)

Daynac et al., (in prep)

- 0-23
- 23-45
- 45-68
- 68-90
- 90-113
- 113-135
- 135-158
- 158-180

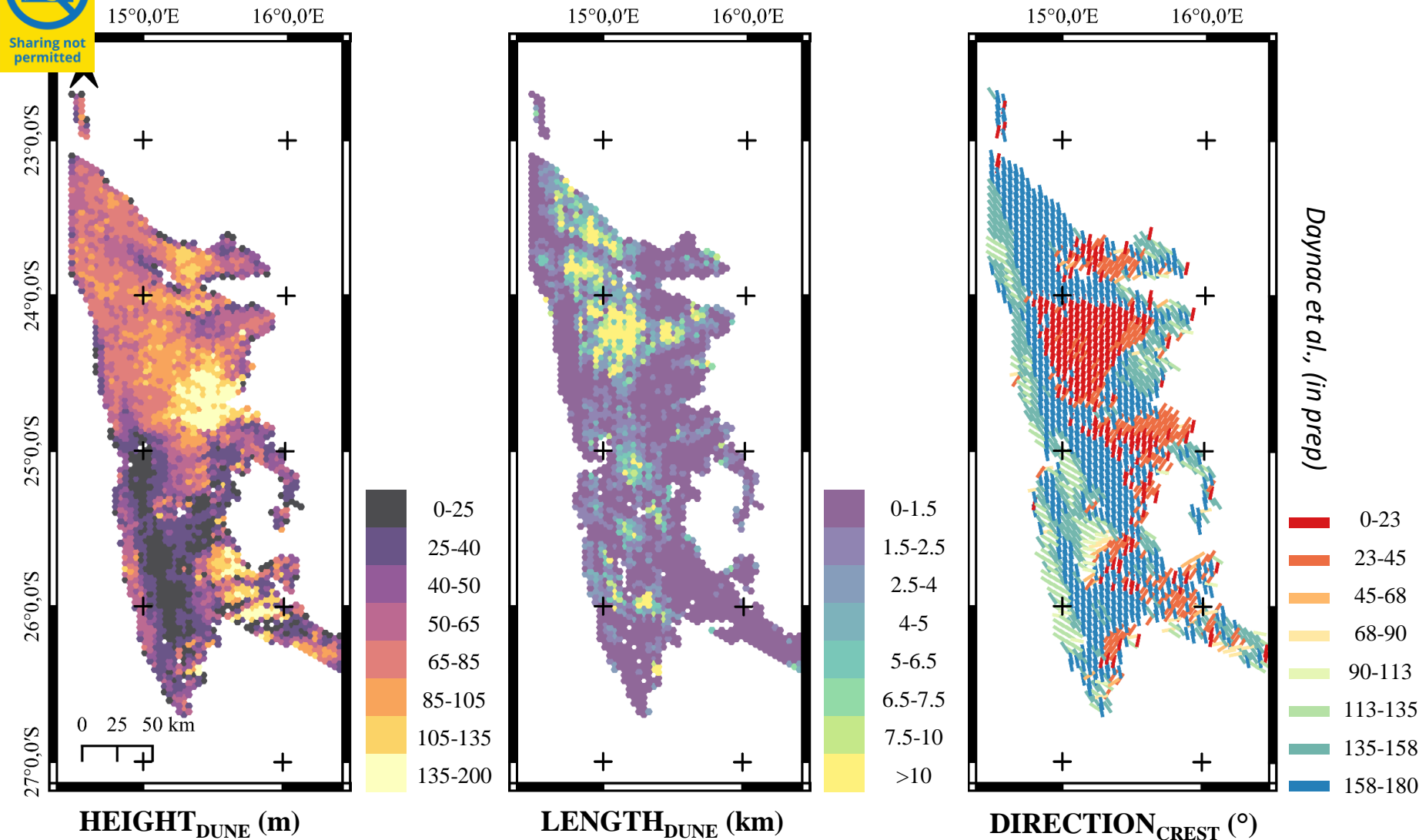
Comparison with current map



modified from Livingstone et al., 2014

Morphometric parameters of Namib dunes


Sharing not permitted



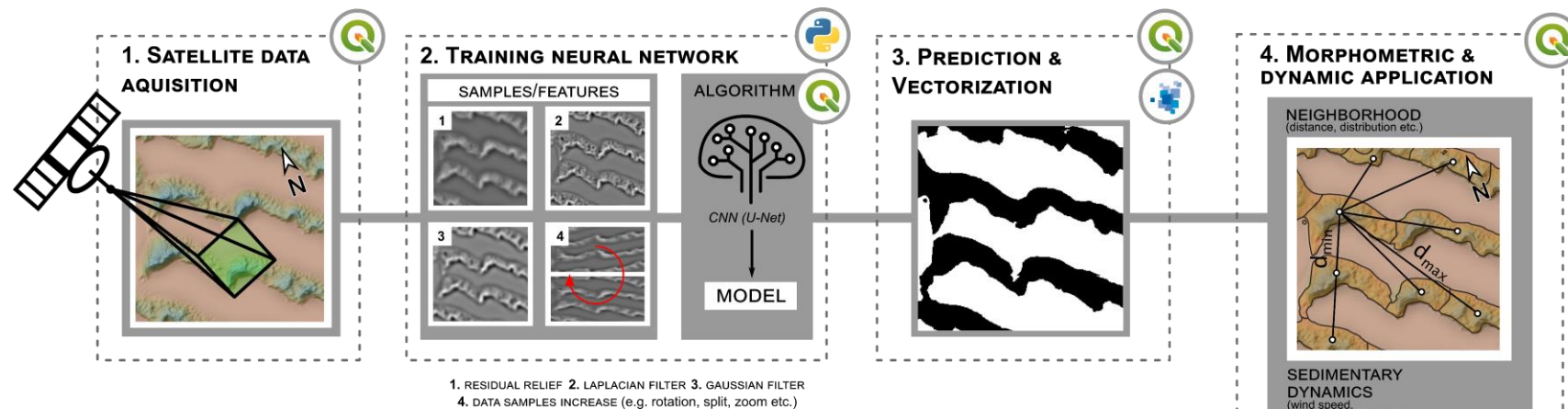
This is one of the first detailed maps of morphometric parameters of the Namib dunes showing:

- Mean crestlines direction of 149°(range: 33°-170°) for very high dunes (>120m) and of 160° (range: 123°-170°) for smaller dunes (<25m);
- An area to the north with a very consistent pattern of long (>10 km) and high (> 80m) dunes with a mean crest direction of 22°;
- A south area with a very consistent pattern of long (7.5 to >10 km) and short (<25 m) dunes with a mean crest direction of 160°;
- A similarity between the different pattern which are highlighted by the morphometric parameters of our work and six dune areas identified at the dune field scale in previous studies:

- Close transverse dunes
- Complex linear dunes
- Compound linear dunes
- Intersecting linear dunes
- Simple linear dunes
- Star and chain of star dunes

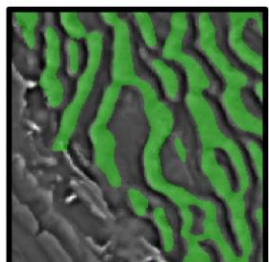
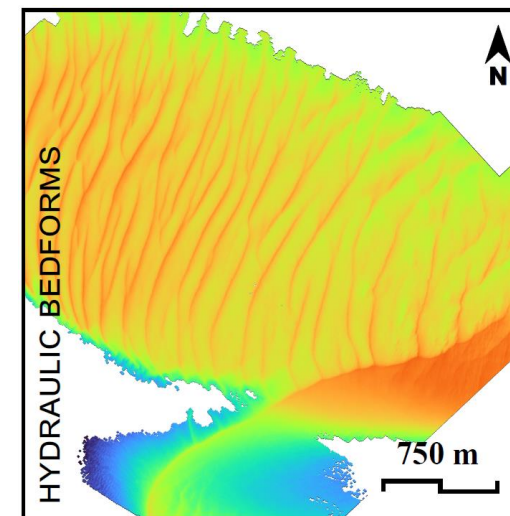
To conclude...

- Efficient semi-automated protocol for producing a large-scale dune databases;
- This work is an original production that completes atlases of these regions present in the literature the morphological boundaries mapped from aerial/satellite images (Barth, 2001; Glennie, 1970; Livingstone et al., 2014; McKee, 1979);
- Only a few detection problems were noticed, and these were caused on by the DEM's resolution limit in a few specific locations, which produced a weak dune signal.



Various future uses:

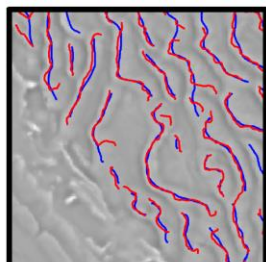
- Use of neighborhood relationships to quantify dune dispersion;
- Use of drift potential relationships, flux calculation, wind speed (Tsoar, 2005; Livingstone, 2007, Ashkenazy and al., 2012, Chanteloube et al., 2022) to identify the sedimentary dynamics of dunes;
- Produce different detailed atlases of aeolian dunes diversity and their morphometric parameters on a global scale;
- Application of the protocol in different environments: hydraulic & extraterrestrial.



RR & GT mask



Automatic shape output



Automatic crest output

**Thank you for your attention and if you
have more questions, contact me:**

`jimmy.daynac@univ-lemans.fr`



Source: <https://wallpapercave.com>

Acknowledgements

Thanks to Samuel Shumack for our collaboration. Thanks to IPGP (Institut de Physique du Globe de Paris) for providing the Namib DEM and for our discussions. This work was supported by the French National program PNP (Programme National de Planétologie).

References

- Ashkenazy, Y., Yizhaq, H., Tsoar, H., 2012. Sand dune mobility under climate change in the Kalahari and Australian deserts. *Clim. Change* 112, 901–923. <https://doi.org/10.1007/s10584-011-0264-9>
- Barth, H.-J., 2001. Characteristics of the wind regime north of Jubail, Saudi Arabia, based on high resolution wind data. *J. Arid Environ.* 47, 387–402. <https://doi.org/10.1006/jare.2000.0668>
- Chanteloube, C., Barrier, L., Derakhshani, R., Gadai, C., Braucher, R., Payet, V., Léanni, L., Narteau, C., 2022. Source-To-Sink Aeolian Fluxes From Arid Landscape Dynamics in the Lut Desert. *Geophys. Res. Lett.* 49, e2021GL097342. <https://doi.org/10.1029/2021GL097342>
- DeLatte, D.M., Crites, S.T., Guttenberg, N., Tasker, E.J., Yairi, T., 2019. Segmentation Convolutional Neural Networks for Automatic Crater Detection on Mars. *IEEE J. Sel. Top. Appl. Earth Obs. Remote Sens.* 12, 2944–2957. <https://doi.org/10.1109/JSTARS.2019.2918302>
- Edgell, H.S., 2006. *Arabian Deserts: Nature, Origin and Evolution*. Springer Science & Business Media.
- Glennie, K.W., 1970. *Desert Sedimentary Environments*. Elsevier Publishing Company.
- Hiller, J.K., Smith, M., 2008. Residual relief separation: digital elevation model enhancement for geomorphological mapping. *Earth Surf. Process. Landf.* 33, 2266–2276. <https://doi.org/10.1002/esp.1659>
- Köhler, M., Shulmeister, J., Patton, N.R., Rittenour, T.M., McSweeney, S., Ellerton, D.T., Stout, J.C., Hüneke, H., 2021. Holocene evolution of a barrier-spit complex and the interaction of tidal and wave processes, Inskip Peninsula, SE Queensland, Australia. *The Holocene* 31, 1476–1488. <https://doi.org/10.1177/09596836211019092>
- Livingstone, I., Baas, A., Bateman, M.D., Bristow, C., Bryant, R.G., Bullard, J.E., Nield, J.M., Thomas, D.S.G., White, K.H., Wiggs, G.F.S., 2014. A prospectus for future geomorphological investigation of the Namib Sand Sea. *Trans. R. Soc. South Afr.* 69, 151–156. <https://doi.org/10.1080/0035919X.2014.936330>
- Livingstone, I., Bristow, C., Bryant, R.G., Bullard, J., White, K., Wiggs, G.F.S., Baas, A.C.W., Bateman, M.D., Thomas, D.S.G., 2010. The Namib Sand Sea digital database of aeolian dunes and key forcing variables. *Aeolian Res.* 2, 93–104. <https://doi.org/10.1016/j.aeolia.2010.08.001>
- Livingstone, I., Wiggs, G.F.S., Weaver, C.M., 2007. Geomorphology of desert sand dunes: A review of recent progress. *Earth-Sci. Rev.* 80, 239–257. <https://doi.org/10.1016/j.earscirev.2006.09.004>
- Lorenz, R.D., Zimbelman, J.R., 2014. *Dune Worlds*, Springer Berlin, Heidelberg. ed. Springer Praxis Books.
- McKee, E.D., 1979. *A Study of Global Sand Seas*. U.S. Government Printing Office.
- Rolland, T., Monna, F., Buoncristiani, J.F., Magail, J., Esin, Y., Bohard, B., Chateau-Smith, C., 2022. Volumetric Obscurance as a New Tool to Better Visualize Relief from Digital Elevation Models. *Remote Sens.* 14, 941. <https://doi.org/10.3390/rs14040941>
- Shumack, S., Hesse, P., Farebrother, W., 2020. Deep learning for dune pattern mapping with the AW3D30 global surface model. *Earth Surf. Process. Landf.* 45, 2417–2431. <https://doi.org/10.1002/esp.4888>
- Tsoar, H., 2005. Sand dunes mobility and stability in relation to climate. *Phys. Stat. Mech. Its Appl., Physics Survey of Irregular Systems* 357, 50–56. <https://doi.org/10.1016/j.physa.2005.05.067>